JOURNAL OF OPTOELECTRONICS AND ADVANCED MATERIALS Vol. 10, No. 5, May 2008, p. 1106 - 1109

Magnetic properties and shape memory effect of Fe-Mn-Cr-Si-R-B ferromagnetic shape memory alloys

T. TODAKA*, M. SONODA, M. ENOKIZONO
[a] *Department of Electrical and Electronic Engineering, Faculty of Engineering, Oita University, 700 Dannoharu, Oita-870-1192, Japan*

This paper presents measured magnetic and shape memory properties of Fe-Mn-Cr-Si-R-B ribbons developed by means of the melt spinning technique in air. Here, R means a rare earth element. The alloys are multi-functional materials, which have both the ferromagnetic property and shape memory property. If we can simultaneously improve the material properties, the applications of the shape memory alloys will be widened dramatically in the field of the electromagnetic sensors and actuators. In order to improve ferromagnetic function of the Fe-Mn-Si based alloys, we have investigated to add rare earth elements. Also we have added Cr and B to improve corrosion resistance and to make ribbon samples directly by means of the melt spinning technique in air. In this paper, measured magnetic and shape memory properties of Fe-Mn-Cr-Si-R-B alloys were compared.

(Received March 13, 2008; accepted May 5, 2008)

Keywords: Ferromagnetic shape memory alloy, Saturation magnetization, Curie point, Magnetic permeability, Austenite finish Point, Fe, Mn-Cr-Si-R-B

1. Introduction

Recently, developments of intelligent materials have been widely investigated in the world. The shape memory alloy is the typical intelligent material, which has both sensing function and actuator function. The shape memory alloys in practical use are Ni-Ti and Cu-based alloys, however they are expensive and paramagnetic materials [1]. Their main applications are antenna elements of mobile phones, eyeglass frames and vestiary fairings. On the other hand, Fe-based shape memory alloys have been widely investigated during the last 25 years because of their low cost, good forming property and high strength [2]. However, the reports on magnetic properties of Fe-based alloys are very few, because the ferromagnetic property and the shape memory property are contrary to each other.

We have focused on Fe Mn-Si based shape memory alloys and investigated to improve ferromagnetic function, to develop multi-functional materials. The Fe-Mn-Si based alloys are paramagnetic materials due to its high manganese content (28-34 Mn, 4-6.5 Si wt%) [3]. In order to improve ferromagnetic function of the Fe-Mn-Si based alloys, we have investigated to add rare earth elements such as Y, Tb, and Pr. Also we have added Cr and B to improve corrosion resistance and to make ribbon samples directly by means of the melt spinning technique in air. Advantage of the melt spinning technique is that we can easily produce a large amount of ribbon and improve shape memory property by changing the crystal condition. As a result, we have found that the saturation magnetization after shape memory treatment increases by adding rare earth elements. Addition of 0.8 - 0.9 wt%Tb was most effective in increasing the saturation magnetization. However, brittleness of the samples was not so good and it was difficult to make ring samples to measure DC magnetic properties [4]. In this paper, the measured properties of the Fe-Mn-Cr-Si-R-B alloys are compared.

2. Sample preparation

In this research, we prepared samples by using the melt spinning technique in air. The melt spinning technique can change the crystal condition from liquid phase to solid phase in a short period in time and achieve a special crystal condition. The procedure of sample production is that an ingot is firstly made with an arc furnace and then ribbons are prepared by using the melt spinning technique. The conditions used in production are that the pressure of Ar gas is 0.1 MPa, the rotation number of a cupper roll is 1800 rpm (20 cm in diameter), and the clearance between a nozzle head and the cupper roll surface is 0.3 mm.

Table 1 shows the chemical component of the prepared samples. We have added 0.5 – 1.0 wt% yttrium, terbium and praseodymium to the base alloy (Fe57.8-Mn26-Cr10-Si6-B0.2). The other components instead of Fe were kept to be constant.

Table 1. Chemical component of the samples [wt%].

Sample	Fe	Mn	Cr	Si	Tb	B
Series-A (R = Y)	57.3	26	10	6	0.5	0.2
	57.2				0.6	
Series-B (R = Tb)	57.1				0.7	
	57.0				0.8	
Series-C (R = Pr)	56.9				0.9	
	56.8				1.0	

The sample ribbons were firstly memorized to be a straight shape with certain heat-treatment called shape memory treatment. In applications of shape memory alloys, the samples need to memorize with the most suitable heat-treatment condition, because the heat-treatment method is different depending on chemical component of samples, shapes and cooling methods. We have tested many heat-treatment conditions such as slow cooling and rapid cooling. Finally, we have selected a rapid cooling method that samples fastened to be straight for 40s at $1000\,^{\circ}C$ in an electric furnace and then rapidly cooled down in water at $20\,^{\circ}C$.

3. Measurement methods

In the evaluation of magnetic properties, we measured the saturation magnetization (Ms emu/g) and the Curie temperature (*Tc* °*C*). The Curie temperature is very important for applications because shape memory alloys return a shape memorized before deformation by heating. The saturation magnetization was evaluated in M-H curve measurement by a vibrating sample magnetometer (VSM). The applied magnetic field was 10 kOe. The Curie temperature was similarly evaluated in M-T curve measurement under the applied magnetic field was 20 Oe. Also DC magnetic relative permeability was measured by using a ring-specimen measurement method.

In the evaluation of shape memory properties, shape memory effect (*SME* %) was measured by a stability measurement method [3]. The ribbon was firstly memorized to be a straight shape with shape memory treatment. Then it was bended to be 45 degrees at mid point in room temperature as shown in Fig. 1. The recovery angle was measured after heating at 300 °*C* for 10s in a muffle furnace. The shape memory effect was calculated by the recovery angle, α.

$$SME = (45 - \alpha)/45 \times 100 \ [\%] \tag{1}$$

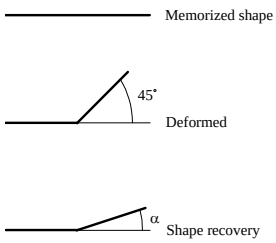

Fig. 1. Evaluation method of SME.

Additionally the shape recovery rate (*SRR* %) was measured in constant stress loading tests with a thermo mechanical analyzer (TMA). The shape recovery rate measurement is a common evaluation method of the shape memory property. The samples were endowed with 1.8 % residual strain by tensile force and then the shape recovery strain was measured with the TMA. The shape recovery rate was calculated by

$$SRR = \frac{\varepsilon_{\mathrm{REC}}}{\varepsilon_{\mathrm{R}}} \times 100 \ [\%] \tag{2}$$

where, ε_{R} and $\varepsilon_{\mathrm{REC}}$ are the residual strain and the shape recovery strain, respectively. Also austenite transformation finish temperature (*Af*) that the shape after deformation completely recovers, was detected from the changes of the strain recovery curves.

4. Measured results

Fig. 2 shows the saturation magnetization and the shape memory effect of the series-A. As shown in Fig. 2 (a), the samples without the shape memory treatment, had higher saturation magnetization over 100 emu/g. However the magnetic property deteriorated after the heat-treatment as shown in Fig. 2 (b). The saturation magnetization in as spun samples was almost constant, and unrelated to change of the yttrium contents. The saturation magnetization after the heat-treatment decreased with increasing yttrium contents.

As for the shape memory effect, the SME was below 40% before the shape memory treatment as shown in Fig. 2 (a). However they showed excellent *SME* (100 %) after heat-treatment as shown in Fig. 2 (b). The 0.5wt%-yttrium sample showed the highest saturation magnetization about 120 emu/g in preserving the perfect *SME* (100%).

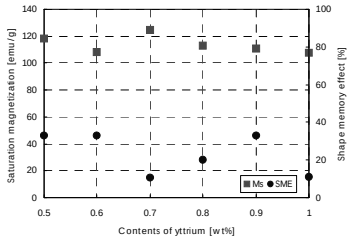

(a) As cast

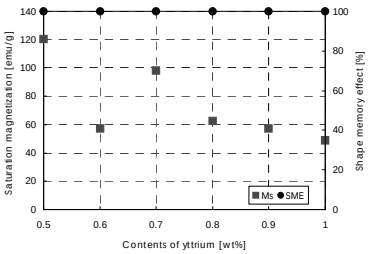

(b) After shape memory treatment

Fig. 2. Saturation magnetization and shape memory effect of Fe-Cr-Mn-Si-Y-B alloys, Series-A (Y).

Figs. 3 (a) and (b) show the saturation magnetization and the shape memory effect of the series-B (Fe-Mn-Cr-Si-Tb-B ribbons). Fig. 3 (a) shows the properties without the shape memory treatment, and Fig.3 (b) shows ones after the shape memory treatment. As shown in Fig. 3 (a), the saturation magnetizations of the ribbon samples were also over 100 emu/g without depending terbium content and the shape memory effects were very small under 40%. After the shape memory treatment, the properties were changed as shown in Fig. 3 (b). All the samples showed the perfect shape memory effect of 100 % after the shape memory treatment, however the saturation magnetizations of lower terbium content samples below 0.6 wt% were reduced in comparison with ones before the heat treatment. The decreasing rates of the saturation magnetizations were negligible within 0.7-0.9 wt% terbium samples. The 0.9wt%-terbium sample showed the highest saturation magnetization about 110 emu/g.

Figs. 4 (a) and (b) show the saturation magnetization and the shape memory effect of the series-C (Fe-Mn-Cr-Si-Pr-B ribbons). As shown in these figures, as spun samples had also larger saturation magnetization, however the residual saturation magnetizations after the heat-treatment were very small below 60 emu/g. All the samples showed the perfect SME after the heat-treatment. In this series, we could not obtain any improvement of the ferromagnetic property.

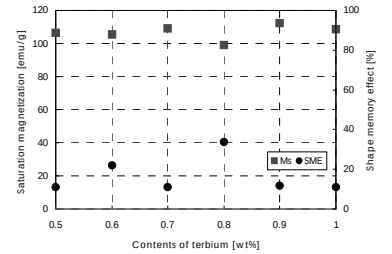

(a) As cast

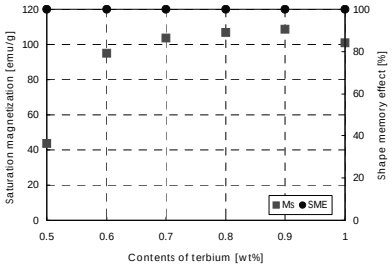

(b) After shape memory treatment

Fig. 3. Saturation magnetization and shape memory effect of Fe-Cr-Mn-Si-Tb-B alloys, Series-B (Tb).

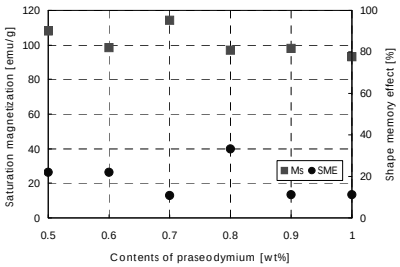

(a) As cast

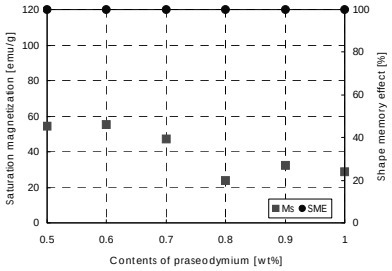

(b) After shape memory treatment

Fig. 4. Saturation magnetization and shape memory effect of Fe-Cr-Mn-Si-Pr-B alloys, Series-C (Pr).

Although the magnetic property and the shape memory property were contrary to each other, we could obtain ribbons, which have the perfect shape memory effect of 100 % and comparatively larger saturation magnetization over 100 emu/g. The ribbon containing terbium showed a stable saturation magnetization over 100 emu/g in comparison with ones containing the other rare earth element [5].

The shape recovery rate (*SRR*) and the austenite transformation finish temperature (*Af*), were measured by the TMA after the constant stress loading test. Tables 2, 3 and 4 show the relationship between the residual strain and the shape recovery rate calculated by (2). The shape recovery strain was within 0.1-0.26% and *SRR* was lower than 36%. The *SRR*s of the series-B containing terbium was larger than ones of the other series. However the shape recovery strain and *SRR* were very smaller than ones of NiTi alloys.

Table 2 Shape recovery rate of the series-A.

Series name	Contents of Y [wt%]	Residual strain [%]	Shape recovery strain [%]	SRR[%]
Series -A	0.5	0.67	0.14	20.5
	0.6	0.56	0.12	21.3
	0.7	0.86	0.13	15.3
	0.8	1.35	0.15	10.7
	0.9	0.58	0.14	23.4
	1.0	0.65	0.14	20.7

Table 3. Shape recovery rate of the series-B.

Series name	Contents of Tb [wt%]	Residual strain [%]	Shape recovery strain [%]	SRR[%]
Series -B	0.5	1.15	0.14	12.5
	0.6	0.60	0.16	26.7
	0.7	0.77	0.17	21.5
	0.8	0.85	0.26	30.7
	0.9	0.34	0.12	35.8
	1.0	0.74	0.13	17.8

Table 4. Shape recovery rate of the series-C.

Series name	Contents of Pr [wt%]	Residual strain [%]	Shape recovery strain [%]	SRR[%]
Series -C	0.5	0.62	0.16	25.0
	0.6	1.44	0.22	15.3
	0.7	0.80	0.10	12.5
	0.8	1.20	0.20	16.6
	0.9	0.99	0.13	12.6
	1.0	0.65	0.19	29.8

Figs. 5 (a), (b) and (c) show the equilibrium phase diagram for the each series. As shown in these figures, the austenite-finish transformation temperature (*Af*) was almost constant. They were about (Y) 237 $^{\circ}C$, (Tb) 225 $^{\circ}C$, and (Pr) 234 $^{\circ}C$, respectively. It was evident that the ferromagnetic austenite-phase existed in the region between *Af* and *Tc* curves. The region was widened in proportion to the terbium contents, however narrowed with increasing yttrium content. The effect of the praseodymium content was very small. The ferromagnetic austenite-phase assisted to increase the saturation magnetization. However brittleness of the samples, which have higher contents of the rare earth elements was not good and it was difficult to make ring samples to measure DC magnetic properties. The reason has not yet fully made clear from the results obtained here, however we can state the occurrence of the slip deformation and the increase of the martensitic-start transformation temperature.

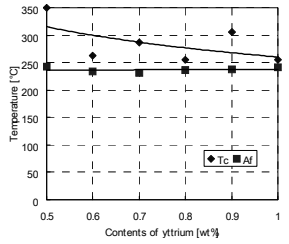

(a) Series-A (Y)

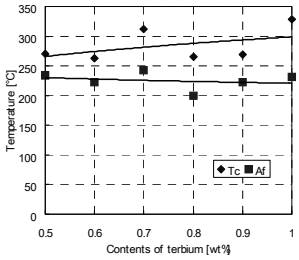

(b) Series-B (Tb)

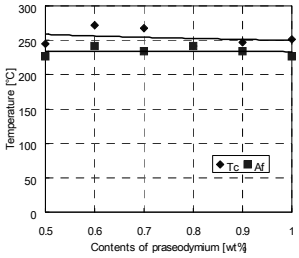

(c) Series-C (Pr)

Fig. 5. Measured Curie temperature (Tc) and the austenite transformation finish temperature (Af).

We also measured the maximum permeability from the initial magnetization curve with a DC magnetization property measurement apparatus. Table 5 shows conditions used in the measurement.

Table 5. Measurement conditions of initial Magnetization curves.

Parameters	Sample with 0.9 wt%Tb
Number of turns of the exiting coil [turns]	208
Number of turns of the B coil [turns]	157
Cross sectional area of the sample [mm^2]	30
Applied magnetic field [Oe]	30

Fig. 6 shows the measured initial magnetization curves of the 0.9wt%Tb sample, which showed comparatively a good magnetic property. The maximum relative permeability of the 0.9 wt%Tb sample was 265. In the measurement of the maximum permeability, we used a ring specimen wound on a cylindrical frame, the brittle ribbons were therefore very difficult to evaluate. Use of the single sheet tester will be more convenient for measurement.

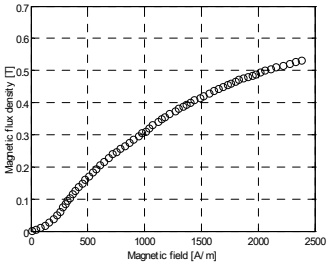

Fig. 6. Initial magnetization curve of the 0.9 wt% Tb sample.

5. Conclusions

In this paper, we have investigated to improve ferromagnetic function of the Fe-Mn-Si based shape memory alloy by adding rare earth elements. As a result, the saturation magnetization increased in a wide range by adding 0.7-1.0 wt%Tb without losing the shape memory properties. The saturation magnetization of 0.9 wt%Tb sample was about 110 emu/g. The maximum relative permeability of the 0.9 wt%Tb sample was about 265. The permeability is small as compared with one of Fe. However, it is applicable level in applications as a core material. The Curie temperature was varied depending on additions. It was evident that the ferromagnetic austenite-phase existed in the region between *Af* and *Tc* curves. The changes of the distance between *Af* and *Tc* curves for rare earth elements was correspond to the amount of the remained saturation magnetization after shape memory treatment. The samples including yttrium below 0.5% should be examined in further measurements.

References

[1] S. Miyazaki, Characteristics and applications of shape memory alloys, 11 (2001).
[2] M. Murakami, H. Otsuka, H. G. Suzuki, S. Matsuda, Complete shape memory in polycrystalline Fe-Mn-Si alloys, Proceeding of ICOMAT-86 (1986).
[3] T. Todaka, T. Yasuoka, M. Enokizono et al., Magnetic properties of iron-based ferromagnetic shape-memory ribbon produced by melt-spinning technique, Journal of Magnetism and Magnetic Materials, **304**, 516 (2006).
[4] T. Todaka, M. Sonoda, M. Enokizono, Magnetic properties of Fe-Cr-Mn-Si-Base ferromagnetic shape memory ribbons, Journal of Magnetism and Magnetic Materials, **310**, 2776 (2007).
[5] T. Todaka, Y. Tsuchida, M. Enokizono, T. Kanada, Development of iron-based ferromagnetic shape memory alloys by means of melt spinning technique, Journal of Advanced Science, **18**, 70 (2006).

*Corresponding author: todaka@cc.oita-u.ac.jp

JOURNAL OF OPTOELECTRONICS AND ADVANCED MATERIALS Vol. 10, No. 5, May 2008, p. 1106 - 1109